# RTE–cNSF: A Hybrid Physics–ML Architecture for Accurate Photon Timing in JUNO

Shengqi Chen[a], Benda Xu[a,b], Qiyu Yan[b,c,d]
on behalf of the JUNO Collaboration

[a]Tsinghua University
[b]University of Chinese Academy of Sciences
[c]University of Warwick
[d]Shanghai Jiao Tong University

16, June 2026

# The Jiangmen Underground Neutrino Observatory (JUNO)

## The Detector

- 20 kton liquid scintillator (LS) target
- Acrylic sphere of 17.7 m radius, with a thickness of 12 cm.
- ∼18,000 20-inch PMTs.

Main physics goal: measure neutrino mass ordering via precise reactor $\bar{\nu}_e$ energy spectrum measurement.

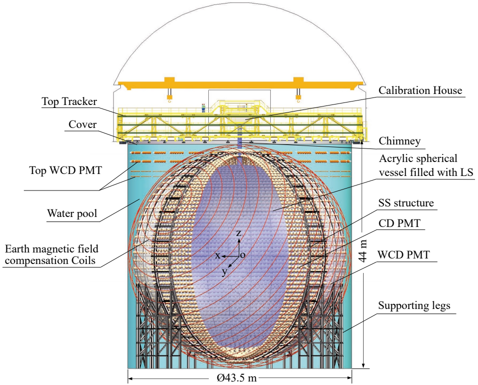

# Challenging Photon Timing

## Photon timing is critical

- Precise energy and vertex reconstruction relies on accurate photon timing.
- Timing affected by complex optical processes: scattering, absorption, re-emission, and reflection.
- GEANT4 provides high-fidelity simulations but is computationally expensive to "fit" optical parameters.

## The gain from differentiable simulation

With a differentiable photon timing model, we can do backpropagation through the likelihood to:

- extract the optical parameters directly from Calibration data (laser, $^{68}$Ge, $\cdots$)
- perform end-to-end fits of physics parameters (vertex, energy) within the same framework.

The gain will be transformative, but how do we build this.

# The Radiative Transfer Equation (RTE)

Instead of tracking individual photons, we model the **photon radiance** and its evolution in space, time:

## Time-dependent RTE / Boltzmann Transport Equation

$$\underbrace{\frac{1}{c}\frac{\partial L}{\partial t} + \hat{s}\cdot\nabla L}_{\text{transport}} + \underbrace{\mu_t L}_{\text{loss}} = \underbrace{S(\mathbf{r}, t, \hat{s})}_{\text{source}} + \underbrace{\mu_s \int f(\hat{s}\cdot\hat{s}')\, L(\mathbf{r}, t, \hat{s}')\, d\hat{s}'}_{\text{in-scatter}}$$

$\mu_t = \mu_a + \mu_s, \;\; \mu_a = 1/L_{\text{abs}}, \;\; \mu_s = 1/L_{\text{scat}}.$

## Source term $S$

Scintillation emitted *isotropically* from vertex $V$:

$$S = \tfrac{Y_{\text{eff}}}{4\pi}\, f_{\text{scint}}(t)\, \delta^3(\mathbf{r} - V)$$

$f_{\text{scint}}$: time PDF (bi-exponential $\otimes$ Gaussian).

## In-scatter term

Photons in direction $\hat{s}'$ redirected into $\hat{s}$ with probability $f(\hat{s}\cdot\hat{s}')$:

- Rayleigh: $f \propto 1 + \cos^2\vartheta$
- Re-emission (isotropic): $f = 1/(4\pi)$

## Key property

The in-scatter term is a **linear** operator on $L$ $\Rightarrow$ the solution is a convergent **Neumann series**.

# Neumann Series Solution

Rewrite as $(\mathcal{T} - \mathcal{K})\, L = S$; formal solution:

$$L = \sum_{n=0}^{\infty} L^{(n)} = \mathcal{T}^{-1} S + \mathcal{T}^{-1}\mathcal{K}\,\mathcal{T}^{-1} S + \mathcal{T}^{-1}\mathcal{K}^2\mathcal{T}^{-1} S + \cdots$$

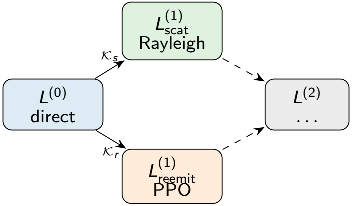


| $n = 0$ | $n = 1$ | $n = 1$ |
|---|---|---|
| direct (ballistic) | Rayleigh scatter | PPO re-emission |

## Implementation strategy

Each term is a separate **precomputed kernel** convolved with the scintillation PDF. Truncate at $n = 1$; Only model single scatter now.

# Boundary — When things gets complicated

## Boundary conditions

The acrylic sphere boundary causes:

- Total internal reflection (TIR) for $\sin\theta_i > n_w / n_{\mathrm{LS}}$.
- Partial Fresnel reflection and refraction for $\sin\theta_i < n_w / n_{\mathrm{LS}}$.
- Reflection at the PMT photocathode, steel frame, $\cdots$.

Introduce late photons, re-distribute photon directions — Need to be modelled.

## TIR is a game changer

Sphere chord identity: angle of incidence preserved on every bounce:
TIR conditions hold for every bounce $\Rightarrow$ photon trapped indefinitely until scatter.

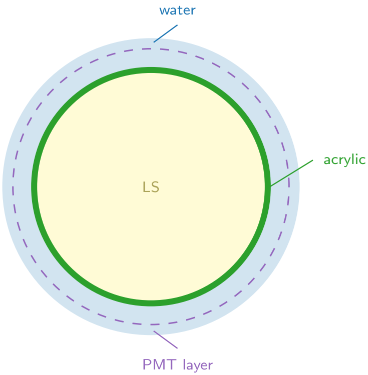


Schematic cross-section of the JUNO detector (not to scale).

# The "dirty" geometry

To model a full sphere detector response like JUNO, we need to capture more than in LS:

## When geometry gets "dirty"

- Photon path intersects the acrylic sphere and water outside $\Rightarrow$ Fresnel reflection/refraction, TIR, multiple bounces.
- Exact ray-tracing beyond the first boundary is messy: many surfaces, many bounces.

## Approach 1: Pure RTE surrogate

- Consider boundary as a special scattering, introducing $L^{(1)}_{\text{boundary}}$ term in the Neumann series.
- Track TIR with a cut-off time, then consider the photon as uniformly leaving the detector.

## Approach 2: Two-stage architecture

- **Our strategy**: Integrate the RTE surrogate without boundary physics, up to the first boundary hit.
- Post-boundary: use machine learning to model the "dirty" photon distribution.

# LS-side: RTE Surrogate

## Neumann series truncated at $n = 1$

$$L = L^{(0)} + L^{(1)}_{\text{Rayleigh}} + L^{(1)}_{\text{re-emit}}$$

- $L^{(0)}$: ballistic — photon travels straight to boundary without scattering.
- $L^{(1)}_{\text{Rayleigh}}$: single Rayleigh scatter en route.
- $L^{(1)}_{\text{re-emit}}$: absorbed then re-emitted by PPO (isotropic).

## Ballistic

Evaluated *directly* at the unique first-hit state:

$$L^{(0)}(B, \hat{s}) \propto \frac{e^{-\mu_t d_{VB}}}{d_{VB}^2}$$

Direction $\hat{s}$ is fixed by geometry $\widehat{VB}$.

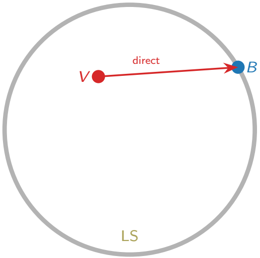

# LS-side: RTE Surrogate

## Neumann series truncated at $n = 1$

$$L = L^{(0)} + L^{(1)}_{\text{Rayleigh}} + L^{(1)}_{\text{re-emit}}$$

- $L^{(0)}$: ballistic — photon travels straight to boundary without scattering.
- $L^{(1)}_{\text{Rayleigh}}$: single Rayleigh scatter en route.
- $L^{(1)}_{\text{re-emit}}$: absorbed then re-emitted by PPO (isotropic).

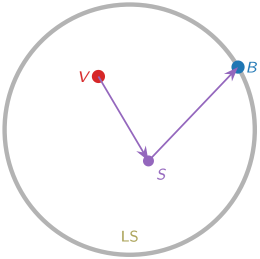


## Ballistic

Evaluated *directly* at the unique first-hit state:

$$L^{(0)}(B, \hat{s}) \propto \frac{e^{-\mu_t d_{VB}}}{d_{VB}^2}$$

Direction $\hat{s}$ is fixed by geometry $\widehat{VB}$.

## Single-scatter

Integrated numerically over $S$ in LS using **QMC** (Sobol):

$$L^{(1)}(R_{\text{src}}, \theta, \alpha_s, \phi_s)$$

Sampled in $(\theta, \phi)$ on sphere and $(\alpha_s, \phi_s)$ exit angles.

# LS-side: RTE Surrogate

## Neumann series truncated at $n = 1$

$$L = L^{(0)} + L^{(1)}_{\text{Rayleigh}} + L^{(1)}_{\text{re-emit}}$$

- $L^{(0)}$: ballistic — photon travels straight to boundary without scattering.
- $L^{(1)}_{\text{Rayleigh}}$: single Rayleigh scatter en route.
- $L^{(1)}_{\text{re-emit}}$: absorbed then re-emitted by PPO (isotropic).

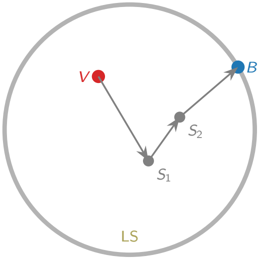


**note**: double scattering not modelled for now.

## Ballistic

Evaluated *directly* at the unique first-hit state:

$$L^{(0)}(B, \hat{s}) \propto \frac{e^{-\mu_t d_{VB}}}{d_{VB}^2}$$

Direction $\hat{s}$ is fixed by geometry $\widehat{VB}$.

## Single-scatter

Integrated numerically over $S$ in LS using **QMC** (Sobol):

$$L^{(1)}(R_{\text{src}}, \theta, \alpha_s, \phi_s)$$

Sampled in $(\theta, \phi)$ on sphere and $(\alpha_s, \phi_s)$ exit angles.

# Results from Approach 1

## Data

Using GhostHunter 2025 competition data[1]: Geant4 simulation with JUNO optical parameters and geometries.

The RTE parameters are fit to the Geant4 MC data.

## Symmetry reduction

Since all geometries are spherically symmetric, the light field only depends on the radial source position $R_{\text{src}}$ and the polar angle $\theta$ of the boundary hit.

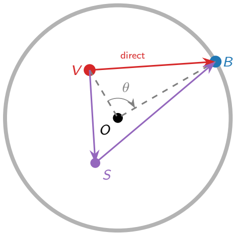


Comparison of the RTE surrogate with Geant4 data at different source positions $R_{\text{src}}$ and boundary angles $\theta$ will be shown in the next slides.

[1] https://ghosthunter.thudep.com/2025/

# Results from Approach 1

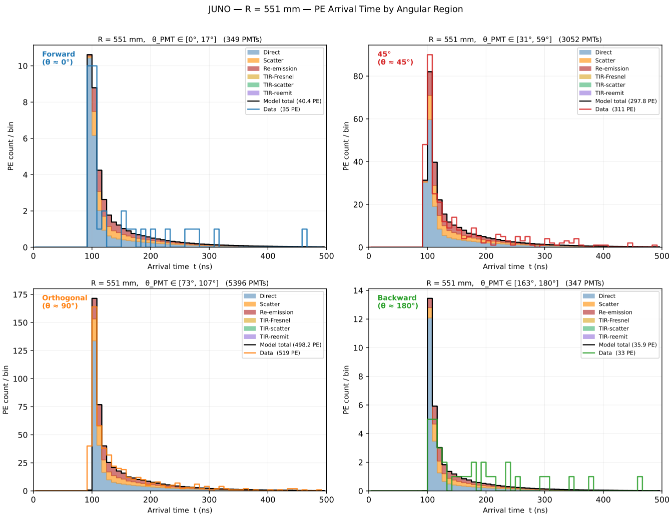


For $R = 551\,\mathrm{mm}$, the RTE surrogate (stacked) shows good agreement with Geant4 (histogram), single scatter term comprehensively captures the late tail.

# Results from Approach 1

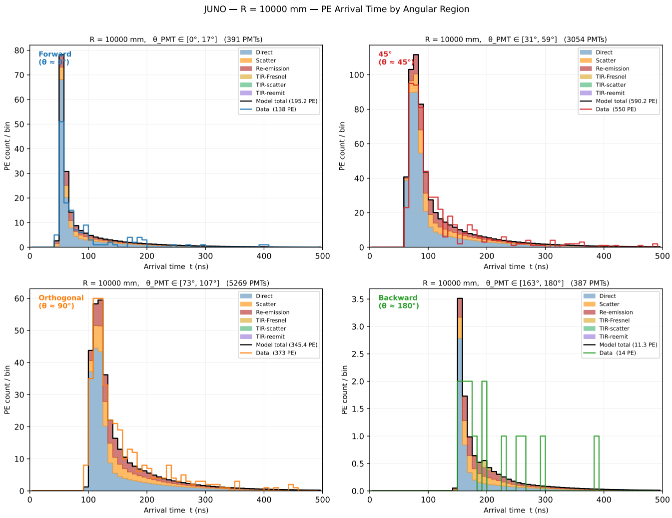


For $R = 10\,000\,\mathrm{mm}$, no significant discrepancy is observed, the RTE surrogate still performs well.

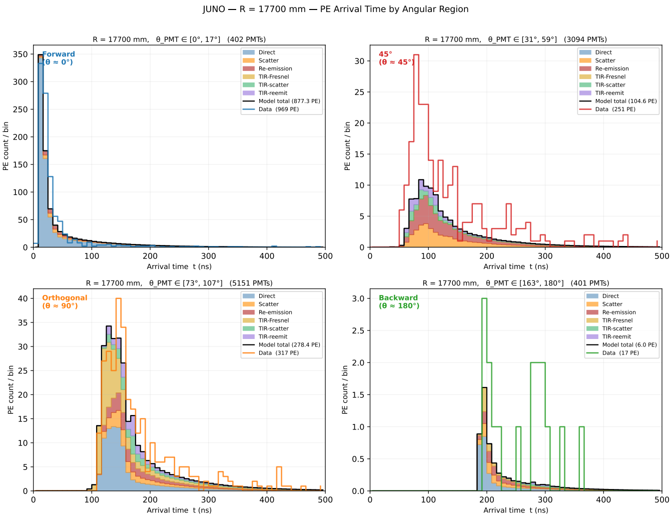


For $R = 17\,700\,\mathrm{mm}$, the RTE surrogate fails to capture the photon contribution in the TIR dominated region ($\theta \approx 45^\circ$), leading to a large discrepancy with Geant4.

# Two-Stage Architecture (for Approach 2)

## Core idea: split at the first boundary

Vertex $V$ in LS $\xrightarrow{\text{RTE surrogate}}$ First-hit boundary $\xrightarrow{\text{NSF timing}}$ Detected PMT hit

## Stage 1: LS-side (RTE)

- Track photon transport *up to* the first boundary (Acrylic-LS) hit.
- Neumann-series surrogate: ballistic + single scatter.
- Output: first-hit boundary state $(B, \hat{s})$.

## Stage 2: Outer-layer (NSF)

- Models all post-boundary physics: Fresnel, TIR, PMT optics.
- Frozen neural spline flow (NSF) learned from Geant4 data.
- Output: timing $T$ at a specific PMT.

## Key interface convention

The LS-side model is responsible only for the *first* hit on the effective boundary. All later reflection / TIR / re-hit histories are absorbed by the outer-layer kernel.

# Outer-layer: cNSF Timing Model

## Frozen conditional kernel

A pre-trained conditioned neural spline flow (cNSF) learns the conditional timing density:

$$p_{\text{cNSF}}(T \mid \theta_1, \theta_2, \phi_1, \ \text{detected})$$

Trained on Geant4 data; **frozen** during downstream fitting.

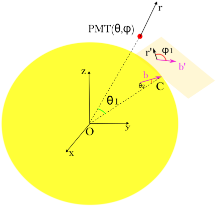


## Condensed geometric variables

3 degrees of freedom due to spherical symmetry:

- $\theta_1$: PMT direction vs. incidence point from detector center.
- $\theta_2$: exit-angle quantity (Snell-mapped from $\alpha_s$).
- $\phi_1$: tangent-plane azimuth of exit direction.

## Key empirical result

When the *true (i.e., detected)* $(\theta_1, \theta_2, \phi_1)$ values are given, the frozen cNSF model can produce **excellent** timing distributions.

$\Rightarrow$ The main challenge is *getting the right boundary measure* into cond-space.

# Full Detected-Hit Model

## Factorized form

The detected-hit distribution factorizes as:

$$p_{\text{detected}}(\theta_1, \theta_2, \phi_1, T) = q_{\text{RTE}}(\theta_1, \theta_2, \phi_1) \cdot \eta(\theta_1, \theta_2, \phi_1) \cdot p_{\text{cNSF}}(T \mid \theta_1, \theta_2, \phi_1)$$

- $q_{\text{RTE}}$: first-hit boundary pushforward measure (from LS-side QMC).
- $\eta$: learned cond-space reweighting / selection factor (i.e., the probability of detection).
- $p_{\text{cNSF}}$: frozen outer-layer timing kernel conditioned on detection.

## Role of $\eta$

$\eta$ is *not* an extra timing model — it is a learned reweighting in cond-space. Current evidence: cNSF kernel is strong but only reveals distribution shape; the gap is the RTE-to-cond pushforward.

# $\eta$ Network: Learning the Detection Probability

## Formulation

$\eta$ is a binary classifier trained on the detected vs. undetected first-hit photon samples, and thus (implicitly) depends on the distribution of first-hit photon roots given by inner layer (RTE or G4)

$$\eta(\theta_1, \theta_2, \phi_1) = P(\text{detected} \mid \theta_1, \theta_2, \phi_1)$$

## Data imbalance

The samples exhibit a **significantly large** negative-to-positive ratio. According to our G4 dataset:

- Out of 202M photons on LS boundary, only 33M are detected by PMTs, 169M are undetected.
- #Positive samples: 33M, #negative samples: $N_{\text{PMT}} \times 2.02 \times 10^8 - 3.3 \times 10^7 \approx 3.55 \times 10^{12}$.
- Negative-to-positive ratio $\approx 1.1 \times 10^5$.

## Training and adjustment

We adjust the actual data ratio to $1:1$ by under-sampling the negative samples and train a Gradient Boosted Neural Network (GBNN). The final logits in $\eta$ is adjusted accordingly.

# Current Status: The RTE solution

## The Baseline

GEANT4 simulation with selection of single-scatter photons that hit the boundary, record its $(\theta_1, \theta_2, \phi_1)$ distribution as the "pushforward" target. Direct comparison without fitting. Liquid scintillator optical parameters fixed to JUNO official MC values.

## Preliminary results (RTE)

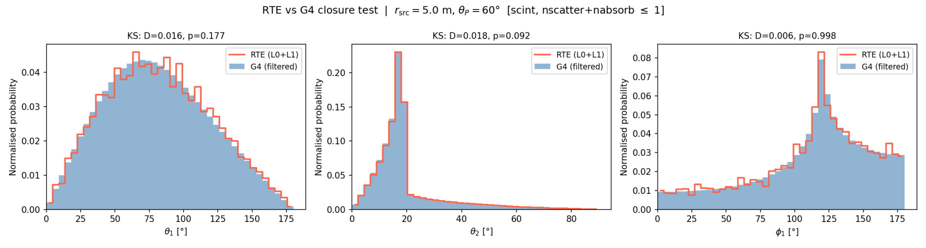


Good consistency between RTE surrogate and Geant4 for the first-hit boundary distribution.

# Current Status: Outer-layer cNSF / $\eta$ Results

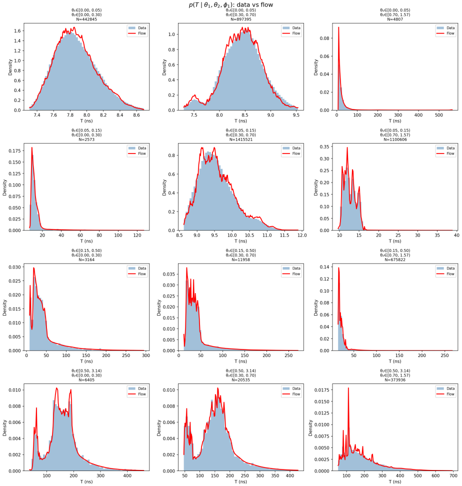


Figure: Conditional histograms of Geant4 detected data (blue shade) v.s. cNSF (red outlines).

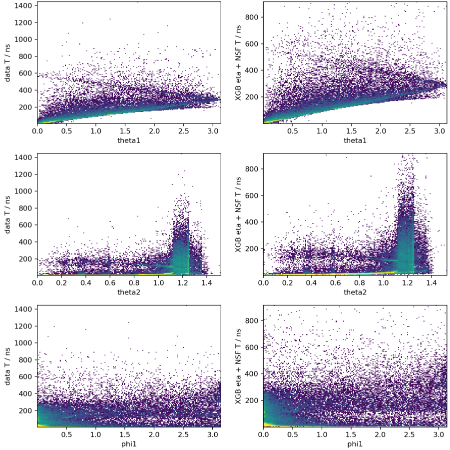


Figure: Marginal distribution of G4 detected data (left) v.s. first-hit samples (from G4) + GBNN $\eta$ + cNSF (right). Shape is similar but scale still mismatches.

# Summary

- Pure RTE surrogate (without NSF) already shows good agreement with Geant4 for the first-hit boundary distribution.
- Using effective boundary condition to model the acrylic sphere is a good first step, but it fails to capture the TIR-dominated region.

## Next steps

- Further train and benchmark the NSF model / $\eta$ network on Geant4 data.
- Integrate and test the full two-stage architecture with the frozen NSF and the RTE surrogate on both Geant4 and real calibration data.

Thanks!

# Term $L^{(0)}$: Direct (Ballistic) Photon

## Geometry

Vertex $V$, PMT $P$ at $R_{\mathrm{PMT}}$, opening angle $\theta$:

$$d_{\mathrm{VP}} = \sqrt{R_{\mathrm{PMT}}^2 + r_v^2 - 2R_{\mathrm{PMT}}\, r_v \cos\theta}$$

$$\cos\alpha = (R_{\mathrm{PMT}} - r_v \cos\theta)/d_{\mathrm{VP}}$$

$$d_{\mathrm{LS}} = \text{path inside LS (Snell)}$$

## Time-integrated yield

$$\lambda^{(0)} = Y_{\mathrm{eff}} \cdot \frac{\cos\alpha}{d_{\mathrm{VP}}^2} \cdot e^{-d_{\mathrm{LS}}/L_{\mathrm{abs}} - d_{\mathrm{LS}}/L_{\mathrm{scat}}} \cdot T_{\mathrm{fr}}$$

## Rate

$$R^{(0)} = \lambda^{(0)} \cdot \left[(1 - f_{\mathrm{bkg}})\, f_{\mathrm{scint}}(t - t_{\mathrm{flight}} - t_0) + \frac{f_{\mathrm{bkg}}}{T_{\mathrm{MAX}}}\right]$$

## Scintillation PDF

Bi-exponential $\otimes$ Gaussian (analytic erfc form):

$$f_{\mathrm{scint}} = f_f\, G(\tau, \tau_f) + (1 - f_f) G(\tau, \tau_s)$$

$$G(\tau, \tau_d) = \tfrac{1}{2\tau_d} e^{\sigma^2/(2\tau_d^2) - \tau/\tau_d} \operatorname{erfc}\!\left(\frac{\sigma/\tau_d - \tau/\sigma}{\sqrt{2}}\right)$$

## 9 free parameters

$Y_{\mathrm{eff}}$, $L_{\mathrm{abs}}$, $L_{\mathrm{scat}}$, $n_{\mathrm{LS}}$, $\tau_f$, $\tau_s$, $f_f$, $f_{\mathrm{bkg}}$, $t_0$. ($T_{\mathrm{fr}} = 0$ at TIR: $\sin\theta_i > n_w/n_{\mathrm{LS}}$.)

# Term $L^{(1)}_{\text{scat}}$: Single Rayleigh Scatter

## Physics

Photon travels $V \to S \to P$. At scatter point $S$:

- Rayleigh phase: $f(\vartheta) \propto 1 + \cos^2 \vartheta$
- Scatter prob.: $\mu_s e^{-\mu_t d_{VS}}$
- Attenuation: $e^{-\mu_t d_{SP}} \cdot T_{\text{fr}}$
- Extra delay: $\Delta t = (d_{VS} + d_{SP} - d_{VP}) n_{\text{LS}}/c$

## Key insight (RTE paper [2401.15698])

For fixed $(V, P, t)$: all scatter points with $d_{VS} + d_{SP} = ct/n_{\text{LS}}$ lie on an **ellipsoid**. The integral reduces to a **1-D integral** over the angle $\varphi$ in the $V$-$P$ plane.

## Precomputed kernel & gradient

Stored: geometry only, binned by $L = d_{VS} + d_{SP}$:

$$g(r_v, \theta_{vp}, L) = \int f(\vartheta)\, \frac{\cos \alpha_S}{d_{SP}^2}\, \delta(d_{VS} + d_{SP} - L)\, d\varphi$$

No $\mu_s$, no attenuation baked in ($\approx$0.4 MB).
At fit time ($\mu_s$, $\rho$ are live JAX params):

$$R^{(1)}_{\text{scat}} \propto \mu_s \sum_k g[\cdots, k]\; e^{-\rho L_k}\; f_{\text{scint}}(t - t_k)$$

$\nabla_{\mu_s}$, $\nabla_\rho$ both flow exactly.

# Term $L^{(1)}_{\text{reemit}}$: Absorption & Re-emission

## Physics (PPO fluorescence)

Photon absorbed at $S$, re-emitted isotropically after lifetime $\tau_{\text{fluor}}$:

- Absorption rate: $\mu_a = 1/L_{\text{abs}}$
- Quantum yield: $Q_{\text{yield}}$
- Direction: isotropic, $f = 1/(4\pi)$
- Delay: $V \to S$ travel *plus* $\tau_{\text{fluor}}$

## Time structure

Re-emission broadens the time distribution:

$$f_{\text{reemit}} = \frac{e^{-\tau/\tau_{\text{fluor}}}}{\tau_{\text{fluor}}} * f_{\text{scint}}(\tau)$$

Explains the heavy late photon tail in data.

## Kernel (same $V \to S \to P$ geometry)

Replace $\mu_s f(\vartheta) \to \mu_a Q_{\text{yield}}/(4\pi)$:

$$h_{\text{re}} = \int \frac{\mu_a Q_{\text{yield}}}{4\pi} e^{-\mu_t(d_{VS}+d_{SP})} \frac{\cos\alpha_S}{d_{SP}^2}\, d\varphi$$

# TIR Kernels: $L^{(1,\mathrm{surf})}_{\mathrm{TIR}}$, $L^{(1,\mathrm{TIR})}_{\mathrm{scat}}$, $L^{(1,\mathrm{TIR})}_{\mathrm{reemit}}$

## $L^{(1,\mathrm{surf})}_{\mathrm{TIR}}$: sub-TIR single bounce

Path $V \to B \to E \to P$ (bounce at $B$, exit at $E$). Bounce points found by Newton iteration on the specular constraint; up to 2 solutions per $(r_v, \theta_{vP})$. Weight: $R_{\mathrm{fr}}(B) \cdot T_{\mathrm{fr}}(E) \cdot \cos\alpha / d^2_{EP}$.

## $L^{(1,\mathrm{TIR})}_{\mathrm{scat/reemit}}$: multi-bounce + scatter

Path $V \to B_1 \xrightarrow{n} \cdots \to S' \to P$.

- $n = 0, 1, \ldots, n_{\max} = 20$ explicit TIR bounces before scatter/reemit at interior point $S'$.
- LS path: $d_{VB} + n \cdot \mathrm{chord}_B + s + d_{S'P}$
- **Geometric tail** ($n > 20$): $q = e^{-\mu_t \cdot \mathrm{chord}_B}$, tail weight $= q^{20}/(1-q)$
- Scatter: prefactor $Y_{\mathrm{eff}}/L_{\mathrm{scat}}$; re-emit: $Y_{\mathrm{eff}} Q_{\mathrm{yield}}/L_{\mathrm{abs}}$

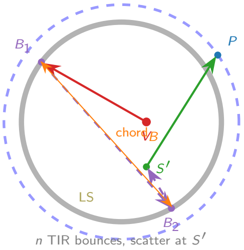

# The JUNO Detector

## Geometry (radii in mm)

| Layer | Boundary |
|---|---|
| Liquid Scintillator (LS) | $r < 17\,700$ |
| Acrylic sphere | $17\,700 \rightarrow 17\,820$ |
| Water buffer | $17\,820 \rightarrow 19\,500$ |
| PMT photocathode | $R_{\mathrm{PMT}} = 19\,500$ |

## Refractive indices

$n_{\mathrm{LS}} = 1.497, \;\; n_{\mathrm{acrylic}} = 1.490, \;\; n_{\mathrm{water}} = 1.340$